Appl. Phys. B 75, 883–890 (2002)
DOI: 10.1007/s00340-002-1060-z

Applied Physics B
Lasers and Optics

B.A. WILLIAMS✉
J.W. FLEMING

Laser-induced fluorescence detection of acetylene in low-pressure propane and methane flames

Chemistry Division, Code 6185, Naval Research Laboratory, Washington, DC 20375-5342, USA

Received: 5 August 2002/Revised version: 30 September 2002
Published online: 20 December 2002 •

ABSTRACT Laser-induced fluorescence is used to detect and record profiles of acetylene formed as an intermediate species in 10-Torr premixed propane and methane flames. In low-temperature regions of the flames, excitation spectra confirm acetylene as the spectral carrier. The spectra of acetylene overlap those of O_2 and NO in terms of both excitation and detection wavelengths, however, acetylene can be detected with relatively little interference in the vicinity of 228 nm, using a detection wavelength of 260 nm. The fluorescence lifetime of acetylene in the flame conditions studied is approximately 20 ns, much shorter than the radiative lifetime, due to a high quenching rate for all the colliders investigated. This can be exploited in low-pressure flames to avoid interference from acetylene in monitoring nitric oxide. The acetylene mole fraction in propane flames reaches its peak value at nearly the same location as that of HCO, slightly closer to the burner than the peak CH mole fraction. The acetylene fluorescence signal is easily detected in propane flames over equivalence ratios from 0.6 to 1.2, although it increases under fuel-rich conditions. In methane flames, the acetylene signal is much weaker and is undetectable for fuel-lean conditions.

PACS 33.50.Dq; 33.50.Hv; 82.80.Dx

1 Introduction

Acetylene occupies an important place in combustion chemistry, both as a fuel itself, and as an intermediate species formed in the combustion pathway of most fuels containing two or more carbon atoms. In spite of its importance, there has been little development of in situ diagnostics for its detection in the reaction zone of flames. Although C_2H_2 was incidentally detected in situ by cavity ring-down spectroscopy near 3200 cm^{-1} in a flame study of the methyl radical [1], it has typically been measured by various techniques (e.g. diode laser spectroscopy [2] or mass spectrometry [3]) following sampling.

Acetylene has been monitored in fuel-rich ethylene flames, with and without acetylene seeding, using coherent anti-Stokes Raman spectroscopy [4, 5]. One limitation of this approach is that CARS inherently has a fairly low sensitivity, making this detection strategy applicable only to environments where there are high acetylene concentrations. Raiche et al. [6] briefly investigated laser excitation of acetylene in low-pressure flames where acetylene was the fuel, and observed fluorescence both from acetylene itself (in the 260–300 nm region) and from C_2 (in the Deslandres–d'Azambuja system from 360–420 nm and the Swan system from 450–600 nm) produced by photofragmentation of the acetylene. They suggested that C_2 photofragmentation fluorescence could be a detection method for acetylene, with the difficulties: 1) the process by which C_2 is produced in excited electronic states following the initial absorption of a laser photon by ground state acetylene is not known; and 2) native C_2 already in the flame contributes a substantial interference signal. Raiche et al. primarily studied C_2 fluorescence, which under their conditions (peak laser intensities ranging from 0.2–2.0 GW/cm^2) gave much stronger signals than the direct C_2H_2 fluorescence.

Here we extend the investigations of Raiche et al., to investigate acetylene fluorescence following excitation at longer wavelengths and lower peak power densities, making secondary photochemical processes less likely. Also, we demonstrate that acetylene can be detected with reasonable signal/noise ratios as an intermediate species formed from both propane and methane fuels. Finally, we document interferences likely to exist between nitric oxide, molecular oxygen and acetylene, all of whose absorption and emission spectra lie in the same wavelength region.

2 Experimental approach

Experiments were conducted in a McKenna flat-flame burner apparatus described previously [7]. A variety of flame conditions (Table 1) were investigated for both methane and propane fuels, with equivalence ratios ranging from 0.6 to 1.2, at a pressure of 10 Torr. Profiles of flame temperature were determined from the rotationally resolved LIF excitation spectrum of the OH radical near 281 nm [7]. The measured temperature values (taken at 14 locations in each flame, typically having uncertainties of 25 K) were used to fit a five-parameter functional form (Table 2). The maximum value of the fitted temperature profile, and its height above the burner, are listed in Table 1.

✉ Fax: +1-202/767-1716, E-mail: brad@code6185.nrl.navy.mil

Fuel	Equivalence ratio	Fuel flow rate (slm)[a]	Oxygen flow rate (slm)	Nitrogen flow rate (slm)	Peak temperature height above burner
Propane	0.6	0.132	1.106	0.439	1719 K @ 1.1 cm
Propane	0.8	0.132	0.819	0.709	1775 K @ 1.2 cm
Propane	1.0	0.160	0.796	0.688	1883 K @ 1.2 cm
Propane	1.2	0.187	0.780	0.672	1984 K @ 1.4 cm
Methane	0.8	0.328	0.819	0.543	1829 K @ 1.3 cm
Methane	1.0	0.400	0.796	0.527	1889 K @ 1.2 cm
Methane	1.2	0.467	0.780	0.515	1986 K @ 1.5 cm

[a] standard (1 atm, 0 °C) liters/minute

TABLE 1 Equivalence ratios, gas flow rates, and peak temperatures as measured using laser-induced fluorescence of the OH radical, for the flames studied. All flames were premixed and stabilized on a round water-cooled burner having a surface area of 28.3 cm^2. All flames were maintained at a pressure of 10 Torr (1.333 kPa). Gas flow rates are specified in standard l/min (l/min at 273 K, 760 Torr (101.3 kPa))

Flame	A (K)	B (dimensionless)	C (cm)	D (cm)	E (K/cm)
Propane 0.6	1803	3.5	−0.15	0.21	62
Propane 0.8	1880	1.5	0.10	0.22	72
Propane 1.0	2015	3.5	−0.10	0.23	90
Propane 1.2	2155	3.5	−0.12	0.27	103
Methane 0.8	1975	1.5	0.13	0.24	95
Methane 1.0	2015	3.5	−0.08	0.21	90
Methane 1.2	2160	3.5	−0.05	0.27	100

Fitted temperature profile parameters:
$T(x) = A/\,(1 + B \times \exp\,(-(x - C)/D)) - E \times x$; T (K), x (cm)

TABLE 2 Functional form and fitted parameters for temperature profiles of flames investigated, fit from 0 to 5 cm above the burner surface

Fluorescence was excited using the frequency-doubled output of a dye laser (Sirah Cobra), pumped by the 3rd harmonic of a Nd:YAG laser (Spectra Physics 170). To access the spectral region between 224 and 235 nm, the dye laser was run using Coumarin 480 dye (Exciton) dissolved in p-dioxane, which has an approximate tuning range from 445 nm to 475 nm, blue-shifted by about 20 nm compared to its tuning range in methanol. This tuning range is very similar to that of Coumarin 460 dissolved in methanol, however Coumarin 480 has better photochemical stability. Typical pulse energies of the doubled dye laser beam were approximately 0.5 mJ in a beam area of 0.25 mm^2, giving a peak power density of approximately 30 MW/cm^2. Fluorescence was collected by a two-lens imaging system, and detected by a Hamamatsu R177 photomultiplier.

For detection of fluorescence from acetylene, nitric oxide and molecular oxygen, an interference filter having a bandwidth (FWHM) of 10 nm and a center wavelength of 262 nm was placed in front of the photomultiplier. Dispersed fluorescence spectra were recorded using a 0.25-m monochromator (Jarrell–Ash) with 0.5-mm slits, resulting in a spectral resolution of approximately 1 nm. Calibration of the monochromator wavelength was accomplished by observation of several mercury lines from 254 nm to 436 nm, as well as scattered laser light (228 nm) in both the first and second orders.

Measurement of fluorescence lifetimes and subsequent determination of quenching cross sections was accomplished using a cold flow of acetylene (passed through a dry ice/ethanol trap to remove acetone) into the burner chamber, together with various mixtures of oxygen, nitrogen, argon and methane. Detection of fluorescence in the quenching studies was accomplished using the monochromator with the slits removed, producing an approximately 20-nm bandpass centered at 260-nm. Fluorescence traces, averaged over 256 laser shots, were digitized on an oscilloscope (Hewlett–Packard Infinium) for determination of fluorescence decay rates. Baseline corrections for the fluorescence signal were made by recording a waveform in immediate succession with the laser beam blocked.

3 Spectroscopy of C_2H_2

3.1 *Excitation spectra*

Various aspects of the spectroscopy of the $\tilde{A}$-$\tilde{X}$ system of acetylene have been extensively studied by a variety of techniques for several decades [8–13]. Acetylene is linear in its electronic ground state, and has a planar trans-bent equilibrium geometry in its lowest excited singlet state [8]. The transition occurs in absorption beginning at approximately 240 nm, and continues for several tens of nm to shorter wavelengths [9]. The spectral transition is forbidden for a linear geometry, and the Franck–Condon factors for absorption in the ground state greatly increase when acetylene is excited in the trans bending mode. For this reason, bands with 1000 cm^{-1} or more of vibrational energy are quite prominent in the absorption spectrum even at room temperature [9]. C_2H_2 has a pre-dissociation threshold (to $C_2H + H$) at slightly higher energy levels in the $\tilde{A}$ state than those accessed here [10].

Figure 1 shows an excitation spectrum recorded in a stoichiometric propane flame at a height of 0.1 cm above the burner. Comparison with the absorption spectrum of acetylene from [9] confirms the identity of C_2H_2 as the spectral carrier. This energy region includes the V_1^2 band, where the symbol V is used to denote the trans bending mode, since the numbering convention for this mode switches between the upper state (ν_3) and the lower state (ν_4) due to the change in point group. Relative intensities of the various rotational lines differ somewhat between the LIF and absorption spectra, in part due to the higher temperature (approximately 700 K at this location for this flame condition, as determined by the OH LIF temperature measurements). Additionally, in a study comparing LIF and absorption spectra of higher energy levels of the $\tilde{A}$ state above the pre-dissociation threshold, Suzuki and Hashimoto [10] found anomalous differences in fluorescence intensities, depending on the rotational level.

For the range of excitation wavelengths between 225 and 235 nm, a number of other vibronic transitions appear, all hav-

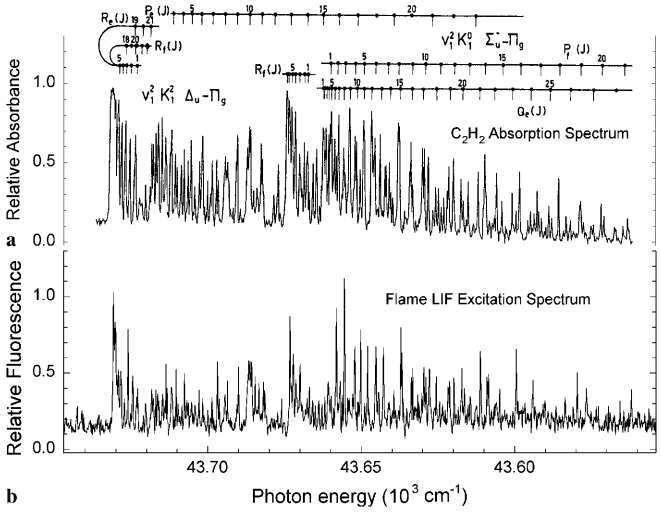

FIGURE 1 **a** Absorption spectrum of room-temperature C_2H_2 from [9]. **b** LIF excitation spectrum in the 10-Torr $\phi = 1.0$ propane flame, at a height of 0.1 cm above the burner

ing the same general appearance as the bands shown in Fig. 1. Some of these are reported in the room-temperature work, while others are not, and probably arise from high-lying vibrational levels of the ground state which are unpopulated at room temperature. Conversely, the bands which appear in both the room-temperature and flame spectra all arise from excited vibrational levels of the $\tilde{X}$ state; bands visible in the room-temperature spectrum arising from the unexcited ground state are not distinguishable. This observation is consistent with the expectation that the transition moment (very small for the non-vibrationally excited ground state) will dominate over the thermal population factor as the temperature is raised. The spectrum in Fig. 1 was recorded as close to the burner as possible to avoid spectral congestion. Spectra recorded higher in the flame (temperatures of 1500–2000 K) still exhibit spectral features suggestive of acetylene, but are highly overlapped. A similar situation was found for the CF_2 radical, which like acetylene possesses several low-frequency vibrational modes and exhibits severe spectral congestion at high temperatures [7].

We used the $2_0^1 V_3^2$ band shown in Fig. 2 (ν_2 is the C−C stretching mode in both the upper and lower states) to record profiles of acetylene concentration in our flames. This band possesses 1850 cm^{-1} of vibrational energy in the ground state, and has a Boltzmann factor which reaches its maximum value at approximately 950 K, making it relatively temperature insensitive over the typical range of temperatures found in flames in converting from fluorescence signal to mole fraction. The rotational assignments shown in Fig. 2 were determined from the energy-level tabulations of [9]; the uncalibrated dye laser wavelength was adjusted (within 2 cm^{-1} of the expected vacuum correction) to match the positions of the R-branch bandheads. The R_f branch bandhead of the K_1^2 subband was used to record LIF profiles (K is the azimuthal angular momentum quantum number when acetylene is treated as a symmetric top; in the linear ground state it arises through excitation of the bending vibrations).

3.2 *Fluorescence spectra*

Figure 3 shows dispersed fluorescence spectra recorded in the $\phi = 1.2$ propane flame from $K' = 2$ subbands of the V^2 and $2^1 V^2$ vibronic levels of the $\tilde{A}$ state, whose excitation spectra are shown in Figs. 1 and 2. O'Brien et al. [11] have published dispersed fluorescence spectra from the $K' = 1$ subbands of these same two vibronic levels; Stephenson et al. [14] have published resolved emission spectra from the $V^i K^1$ levels ($i = 0, 1, 2$). As seen in Fig. 3, fluorescence occurs to a large number of ground-state vibrational levels, showing long progressions in the C−C stretching and trans bending modes [11]. Strong emission

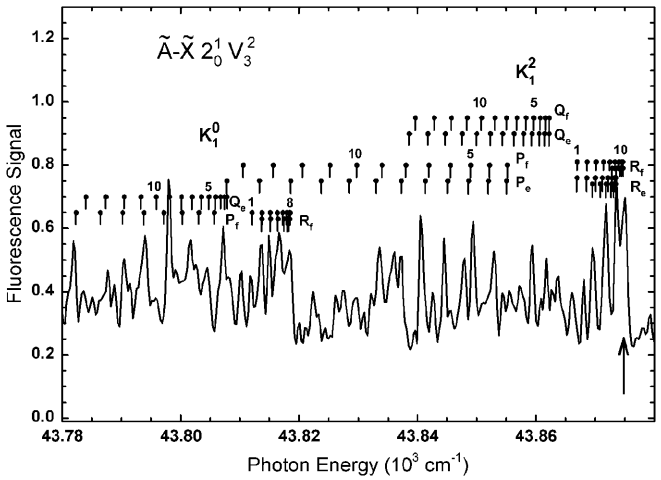

FIGURE 2 Excitation spectrum of the acetylene $\tilde{A}$-$\tilde{X}$ $2_0^1 V_3^2$ band recorded in the 10-Torr $\phi = 1.0$ propane flame. Line positions are shown for selected branches of the band; transition energies were calculated from the energy-level tabulations given in [9]. The spectral feature used to obtain profiles shown below is indicated with an *arrow*

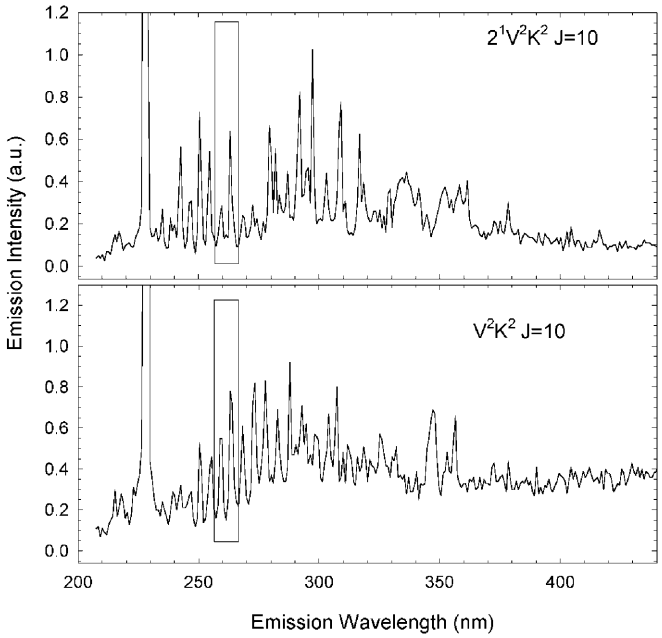

FIGURE 3 Dispersed fluorescence spectra of acetylene in a 10-Torr $\phi = 1.2$ propane flame from the indicated $\tilde{A}$-state energy levels. The *rectangles* indicate the bandpass of the interference filter used to record excitation spectra and flame profiles

bands range from 3000 to 15 000 cm^{-1} of ground-state internal energy (240–350 nm fluorescence wavelength), with the spectrum becoming very congested above 10 000 cm^{-1} (300 nm).

The general appearance of the dispersed fluorescence spectrum in Fig. 3 is similar to those presented in [10], with one noteworthy difference. The relative intensities of the emission peaks is markedly different between the $K' = 2$ levels in Fig. 3 and the $K' = 1$ levels in [11] and [14]. This phenomenon arises due to the approximate observation of the $\Delta K = \pm 1$ selection rule [10], together with the fact that odd (even) levels of the ground-state trans bending mode only give rise to odd (even) values of K''. Thus, fluorescence from an odd (even) level of K' is most prominent to even (odd) ground-state trans bending levels. The different pattern of intensity alterations between the $K' = 1$ and $K' = 2$ dispersed fluorescence spectra is most apparent at low internal energies, where the ground-state vibrational structure is relatively uncongested. For both upper state levels, whose spectra are shown in Fig. 3, two reasonably strong fluorescence features lie within the bandpass of the 262-nm interference filter used to record excitation spectra and flame profiles. For excitation of the $2^1_0 V^2_3$ band, the difference in photon energies between the excitation and fluorescence wavelengths, together with the initial vibrational excitation, gives approximately 7000 cm^{-1} of internal energy following fluorescence.

3.3 *Fluorescence lifetime and quenching*

The radiative lifetime of the acetylene $\tilde{A}$ state below the pre-dissociation limit is of the order of 300 ns [10, 14]. In the flame experiments, however, we find a very short fluorescence lifetime of approximately 20 ns, only slightly longer than the temporal resolution afforded by the laser pulse length and the response time of the photomultiplier. Since both the excitation and emission spectra are consistent with assignment to acetylene and not to any possible photofragment, it is likely that a high quenching cross section is responsible for the short fluorescence lifetime. Raiche et al. [6] reported a high quenching coefficient of approximately 5×10^{-10} cm^3/s in an acetylene/oxygen flame when the V^3 level was pumped.

Quenching cross sections for the $\tilde{A}$ state of acetylene (at room temperature) have been measured for various colliders, including H_2, N_2, O_2, C_2H_2 and CO_2 [14–16]. Stephenson et al. [14] found that the cross sections for quenching by He, Ar, N_2 and O_2 for the V^2K^1 level all ranged from $2–3 \times 10^{-10}$ cm^3/s. For the latter three colliders, the quenching rate was between 80% and 90% of the hard sphere collision rate. For the V^0K^1 and V^1K^1 levels, the quenching rates were much lower and a greater difference was found between colliders. Wolff and Zacharias [16] noted substantial variations in the self-quenching coefficient of acetylene as a function of rotational level for the V^0K^1, V^1K^1 and V^2K^1 levels of the $\tilde{A}$ state. To our knowledge, quenching from $\tilde{A}$ state levels having values of K' other than 1 has not been reported.

We have measured fluorescence lifetimes (Table 3) for various mixtures of C_2H_2, N_2, O_2, Ar and CH_4 while pumping the $V^2_1K^2_1R$ bandhead ($J = 9$). Argon was mixed with the acetylene/oxygen mixture primarily to limit its flammability. Previous studies of acetylene quenching have found a bi-exponential decay, with the fluorescence having two components with a "fast" and a "slow" decay rate [14, 15]. The bi-exponential behavior was not apparent for our conditions, probably because the high quenching rate in the present experiment caused the fluorescence quantum yield for the "slow" decay to be extremely low. Therefore the fluorescence was fit to a single exponential decay.

Quenching rates for all the colliders were determined by simultaneously fitting the fluorescence decay for all conditions (Table 3), using the quenching rates for all colliders (including acetylene) as well as the collisionless decay rate, as adjustable parameters in the fit. The last two columns in

P_{total} (Torr)	$P_{C_2H_2}$ (Torr)	Collider No. 1 (pressure)	Collider No. 2 (pressure)	Measured decay rate (10^7 s^{-1})	Fitted decay rate (10^7 s^{-1})
2.80	0.167	N_2 (2.59 Torr)	–	2.43	2.36
3.00	0.158	N_2 (2.45)	CH_4 (0.39 Torr)	2.64	2.53
3.16	0.149	N_2 (2.31)	CH_4 (0.70)	2.78	2.66
3.33	0.142	N_2 (2.21)	CH_4 (0.98)	2.81	2.80
3.55	0.139	N_2 (2.15)	CH_4 (1.26)	2.85	2.98
3.70	0.133	N_2 (2.06)	CH_4 (1.50)	3.12	3.10
1.45	0.362	N_2 (1.09)	–	1.19	1.16
1.81	0.264	N_2 (1.55)	–	1.49	1.52
2.09	0.216	N_2 (1.87)	–	1.75	1.78
2.39	0.191	N_2 (2.20)	–	2.01	2.03
2.67	0.174	N_2 (2.50)	–	2.23	2.26
2.97	0.163	N_2 (2.81)	–	2.39	2.50
3.40	0.135	Ar (3.27)	–	2.40	2.38
3.69	0.130	Ar (3.15)	O_2 (0.41)	2.59	2.64
3.97	0.127	Ar (3.08)	O_2 (0.77)	2.90	2.88
4.21	0.123	Ar (2.98)	O_2 (1.10)	3.10	3.10

Derived quenching coefficients $\pm 1\sigma$(10^{-10} cm^3 s^{-1}):

CH_4	2.3 ± 0.5
N_2	2.4 ± 0.3
Ar	1.9 ± 0.5
O_2	2.5 ± 0.3

TABLE 3 Fluorescence lifetime measurements of acetylene from the V^2K^2 ($J = 9$) state at room temperature for various gas mixtures. Quenching coefficients for N_2, Ar, CH_4 and O_2 (*column 6*) were derived by a least-squares fitting of the fluorescence lifetime measurements

Table 3 show the measured fluorescence lifetimes and those predicted from the fitted quenching rates. Since the acetylene partial pressure was kept nearly constant for all the runs, the acetylene quenching coefficient and the collisionless decay rate could not be independently determined to reasonable accuracy. However, the sum of the two effects ($3.2 \pm 1.5 \times 10^7$ for an acetylene partial pressure of ~ 150 mTorr) is consistent with the radiative lifetime and self-quenching measurements for the $K' = 1$ subband for this vibronic level.

The quenching rates in Table 3 for nitrogen, oxygen and argon all agree, within the combined uncertainties, with the values measured by Stephenson et al. [14] for $K' = 1$. The quenching rate we measure for methane, which had not been previously reported, is similar to those of the other three colliders. It thus seems that acetylene in the V^2 state has a quenching rate which approaches the collision rate for most colliders, except helium [14]. If one assumes an average quenching rate for all species in the flame of 2.4×10^{-10} cm^3/s (average of the measured values for N_2, O_2 and CH_4) and a radiative lifetime of 300 ns, the fluorescence decay rate at 10 Torr would be approximately 25 ns. Since this value is consistent with our observations, the quenching cross sections for other major flame species such as CO, CO_2 and H_2O, which have not been reported for the V^2 level, are also probably close to the collision rate.

Although the high quenching rate for this upper state level in acetylene will drastically limit the fluorescence quantum yield at higher pressures, it actually simplifies the quenching corrections, if the quenching cross sections are relatively temperature independent. Since all colliders investigated have comparable quenching coefficients, determination of the overall quenching rate requires knowledge only of the number density of colliders, not their composition. Since the room-temperature measurements of quenching coefficients of the V^1 state are roughly a factor of five lower than those of the V^2 state, extension of the LIF diagnostic to atmospheric pressure may be possible by using a lower-lying level of the upper state. This scheme does carry two disadvantages: 1) the transition moment is smaller for lower levels of bending excitation in either the upper or lower states, and 2) for the V^1 and V^0 levels, far more difference is observed in quenching cross sections between colliders, requiring knowledge of the local gas composition to make quenching corrections. The temperature dependence of the quenching rate requires investigation, particularly for the lower-lying vibronic levels of the excited state.

3.4 *Intensity dependence*

We find a dependence of the $\tilde{A}\,2^1\,V^2K^2$ acetylene fluorescence signal on laser power (intensities ranging from 2 to 40 MW/cm^2), exhibiting a power-law exponent of 0.73 ± 0.03. Raiche et al. [6] has reported that the laser intensity dependence of the C_2H_2 signal "is slightly less than linear between approximately 0.2 and 2.0 GW/cm^2" for excitation of the V^4 upper state level. The power-law exponent of less than unity could indicate either that the transition is partially saturated, or that subsequent absorption from the acetylene state has a significant effect on the apparent intensity dependence. The fluorescence signal was fairly weak even at the highest laser power used in our experiment, so it was judged unfeasible to reduce the laser intensity still further to find a region of linear intensity dependence.

4 Flame profiles of acetylene

The R-branch bandhead of the $\tilde{A}$-$\tilde{X}\,2^1_0\,V^2_3$ band was used to record LIF profiles for a variety of flame conditions. This feature has 1960 cm^{-1} of thermal energy in the lower state, and thus has a relatively weak dependence on temperature in the range of typical flame temperatures; with the Boltzmann fraction (the fraction of the acetylene molecules which reside in the proper initial state to allow excitation via the spectroscopic transition employed) reaching its maximum value at approximately 1250 K. At higher temperatures, the Boltzmann factor decreases due to the rapid increase in the partition function with temperature.

In the spectra, it was noted that the off-resonance signal never dropped to zero, so that fluorescence was also originating from additional states of acetylene, presumably with higher levels of thermal excitation. This behavior is typical in flame spectra of polyatomic species [17], but must be considered in converting a LIF signal to acetylene concentration.

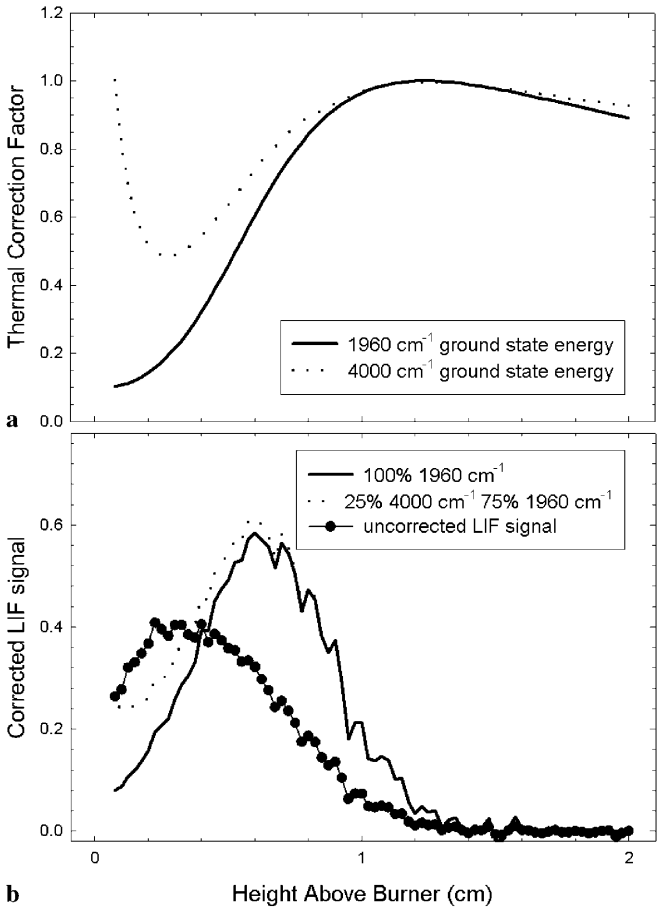

FIGURE 4 **a** Thermal correction factors for the $\phi = 1.0$ propane flame for ground-state thermal excitations of 1960 cm^{-1} and 4000 cm^{-1}. **b** Conversion of the LIF signal into C_2H_2 mole fraction assuming: 1) that all of the LIF signal is due to excitation of the $\tilde{A}$-$\tilde{X}\,2^1_0\,V^2_3$ band (*solid line*); and 2) that 25% of the LIF signal at 0.1-cm height is due to unresolved excitation having a thermal energy of 4000 cm^{-1} (*dotted line*)

In Fig. 4, the effect of having an unresolved background with a thermal energy of 4000 cm^{-1} is investigated. This value of thermal energy was chosen as it represents a reasonable value for the higher levels expected to be thermally populated at flame temperatures of < 2000 K. In the top plot, the thermal correction factors for lower state energies of 1960 cm^{-1} and 4000 cm^{-1} are plotted against distance above the burner for the stoichiometric propane flame, using the measured temperature profile and calculations of the partition function vs temperature under the rigid-rotor harmonic-oscillator approximation. The LIF signal is divided by the thermal correction factor, proportional to the Boltzmann factor divided by the absolute temperature, to yield the relative mole fraction. The rather complicated dependence of the thermal correction factor vs flame position for the 4000 cm^{-1} thermal energy is due to both the temperature as a function of flame position and the correction factor as a function of temperature reaching maximum values at temperatures which differ by about 800 K. The temperature corrections for the two thermal energies are only drastically different within the first 5 mm above the burner.

The lower plot of Fig. 4 shows the uncorrected LIF profile for the propane $\phi = 1.0$ flame, along with the temperature-corrected profile of acetylene mole fraction, under two assumptions. The dotted line is the mole fraction profile assuming all the fluorescence signal comes from states having an initial energy of 1960 cm^{-1}. The solid line is the mole fraction profile derived under the assumption that 25% of the fluorescence signal at 0.1 cm above the burner is derived from molecules having 4000 cm^{-1} of thermal energy. Again, only in the region within the first few millimeters above the burner does the species profile shape exhibit significant sensitivity, to which temperature dependence is assumed. In the profiles discussed below, the temperature correction corresponding to 1960 cm^{-1} of thermal energy has been used.

Figure 5 compares the acetylene profile with those of CH and HCO in the stoichiometric propane flame. The CH radical was monitored using the same detection scheme employed in [7], while the HCO detection scheme is very similar to that described in [17]. In Fig. 5, the profiles of all three species have been converted into relative mole fraction by correcting for variations in number density and Boltzmann fraction with temperature, as described above for acetylene. The acetylene peak occurs slightly before the CH peak, and nearly coincides with that of HCO. Since CH and HCO are often used as markers for the reaction zone of flames, the acetylene profile therefore has the typical appearance of an intermediate species. The acetylene concentration stays at a significant value just above the burner, unlike that of HCO. This observation matches the predictions of flame models, which often show significant concentrations of stable species just above the burner surface, while radical species are depleted by recombination in this low-temperature region.

Figure 6 shows profiles of the acetylene LIF signal (top panel) and mole fraction (bottom panel) for methane flames having equivalence ratios from 0.8 to 1.2, and propane flames having equivalence ratios from 0.6 to 1.2. The mole fraction profiles are given on a relative basis, but are directly comparable between the different flame conditions. For both fuels,

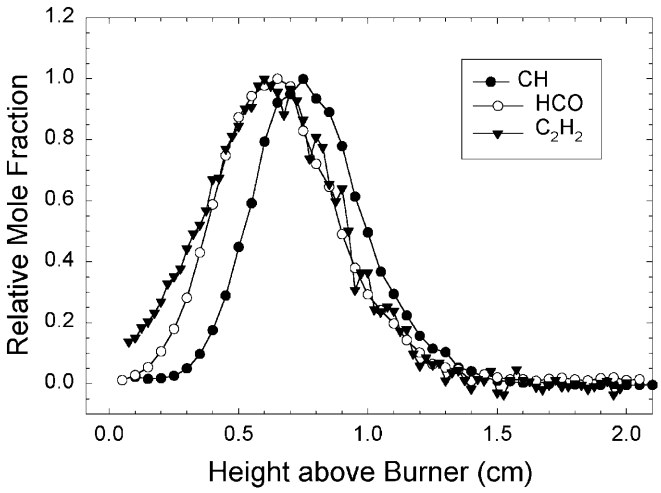

FIGURE 5 Comparison of profiles of CH (recorded by exciting the B-X(0,0) Q_1 (6) line at 389.8 nm), HCO (excited on the $\tilde{B}$-$\tilde{X}$ (002)(000) $^QR_1$ (18) line at 245.5 nm), and C_2H_2 (excited on the spectral feature shown in Fig. 2) in the 10-Torr $\phi = 1.0$ propane flame. All mole fractions (LIF signals corrected for temperature) have been normalized to a maximum value of unity

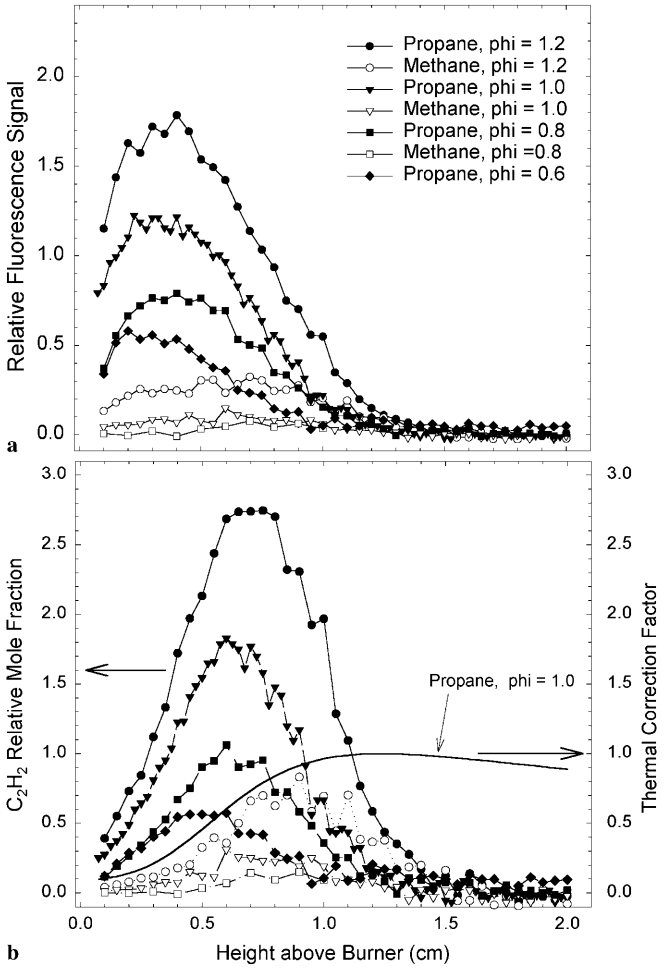

FIGURE 6 Profiles of uncorrected acetylene LIF signals (**a**) and acetylene mole fraction (**b**) obtained by correcting for changes in density and Boltzmann factor as a function of temperature. The correction factor profile (which is multiplied by the LIF profile to obtain the relative mole fraction) for the stoichiometric propane flame is plotted on the *bottom panel* as a *solid line*; the correction factor varies slightly between flame conditions

signal levels increase with increasing equivalence ratio. Signal levels are much larger in the propane flames, where the dependence on equivalence ratio is fairly weak. In the methane flames, there is an easily detected signal for an equivalence ratio of 1.2 (albeit much weaker than in the propane flame of the same equivalence ratio), but the fluorescence is barely discernable for an equivalence ratio of 1.0 and undetectable for an equivalence ratio of 0.8.

The flame observations support the assignment of the LIF signal to acetylene, since C_2H_2 is thought to be formed as one of the key intermediates in the pyrolysis of propane and other "large" hydrocarbons, regardless of flame stoichiometry. In the methane flames, by contrast, acetylene (or any other C_2 species) can only be formed via recombination of C_1 radicals, and thus is only present in significant quantities under fuel-rich conditions.

5 Discussion of interferences

Westblom et al. [18] studied a number of species by LIF in propane flames with and without a manganese-containing fuel additive (MMT—manganese methylcyclopentadienyl tricarbonyl), whose presence was found to have no detectable effect on the concentration of any species monitored. They remarked on photochemical interferences observed in detection of a number of species, including CO and NO, both of which were excited in their study in the same wavelength interval used to record the acetylene spectra shown here. The interference was present only in the reaction zone, and had a peak approximately 1–2 mm closer to the burner than the CH peak. It appears likely that C_2H_2 might have been responsible for the interference observed in NO detection, and that photofragment fluorescence of C_2 could have been responsible for interference observed in CO detection, since the CO detection scheme used a focused laser beam and monitored two-photon excited fluorescence of CO in the same spectral region as the Swan bands of C_2. In fact, we were led to investigate the LIF of acetylene while recording profiles of O_2 using one of the lines of the B-X(2,4) band located in this region. The O_2 profiles showed an obvious interference in the reaction zone, having a similar profile shape to that observed by Westblom et al.

Figure 7 shows spectral scans recorded under identical detection conditions, for different flame conditions and locations. The upper panel, recorded early in the reaction zone of the propane flame with an equivalence ratio of 0.6, shows the spectrum of molecular oxygen, with an underlying congested spectrum ascribed to acetylene. The middle panel shows the post-flame region of the same flame, showing a much cleaner spectrum of oxygen. The lower panel shows a spectrum recorded in the post-flame region of the propane flame with an equivalence ratio of 1.2. This spectrum contains essentially no oxygen or acetylene, but a substantial concentration of NO. The NO concentration is predicted by kinetic models to increase by approximately an order of magnitude from the $\phi = 0.6$ to the $\phi = 1.2$ flame. This is due to both the increase in the CH concentration, leading to an increase in the prompt NO mechanism, and the higher temperature, causing the thermal NO (Zeldovich) mechanism to contribute as well.

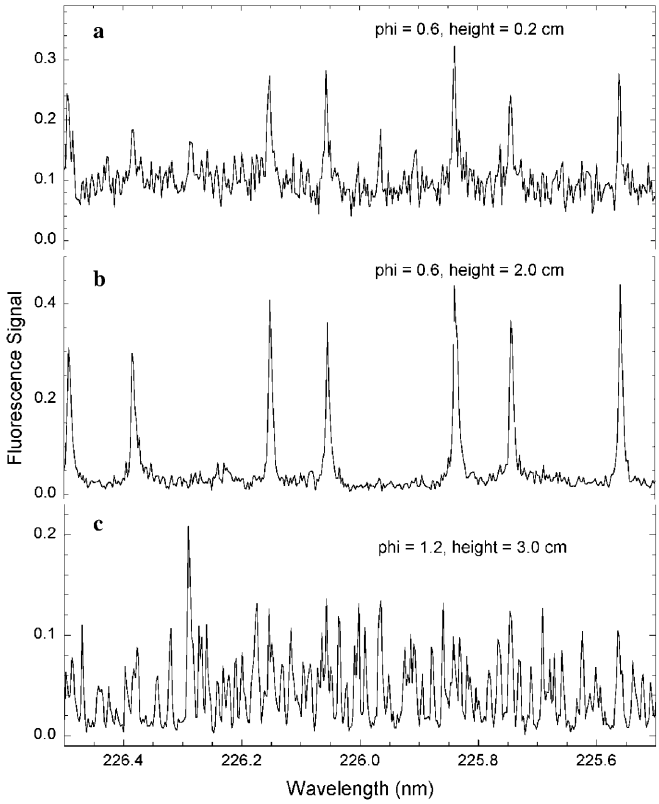

FIGURE 7 Comparison of spectral scans for propane flames at various positions and stoichiometries, showing: **a** the acetylene spectrum underlying the B-X(2,4) band of molecular oxygen; **b** the oxygen spectrum in the absence of acetylene; and **c** the A-X(0,0) band of nitric oxide. All spectra were recorded in immediate succession using the 10-nm bandpass filter centered at 262 nm

We have found that, due to the short fluorescence lifetimes of both O_2 and acetylene, nitric oxide can be detected in propane flames without any discernable interference by delaying the integration gate of the boxcar integrator by approximately 15 ns. Although this strategy is feasible in low-pressure flames, it has the disadvantage of increasing the sensitivity to quenching corrections, and will not be applicable at atmospheric pressure, since the fluorescence lifetime of essentially all species will be less than the pulse width of a nanosecond laser. For monitoring O_2, which has a short fluorescence lifetime due to a pre-dissociative upper state, it is necessary to perform an "on-resonance/off-resonance" subtraction. Since the acetylene spectrum forms a quasi-continuum above roughly 1500 K, this strategy may also be applicable to NO detection at higher pressures.

6 Conclusions

The present work constitutes the first detection, of which we are aware, of acetylene formed as a combustion intermediate by laser-induced fluorescence. The ability to monitor acetylene with a non-intrusive diagnostic will aid validation of kinetic modeling of higher hydrocarbons in which acetylene plays an important role. At the same time, optical diagnostics of nitric oxide or other species excited in this wavelength region must be performed with care under conditions where substantial concentrations of acetylene are likely to be present.

ACKNOWLEDGEMENTS We thank K. Smyth and D. Crosley for helpful discussions. This work was funded by the Office of Naval Research through the Naval Research Laboratory.

REFERENCES

1 J.J. Scherer, K.W. Aniolek, N.P. Cernansky, D.J. Rakestraw: J. Chem. Phys. **107**, 6196 (1997)
2 M.P. Tolocka, P.B. Richardson, J.H. Miller: Combust. Flame **118**, 521 (1999)
3 P.R. Westmoreland, J.B. Howard, J.P. Longwell: Proc. Combust. Inst. **21**, 773 (1986)
4 R.L. Farrow, R.P. Lucht, W.L. Flower, R.E. Palmer: Proc. Combust. Inst. **20**, 1307 (1984)
5 R.P. Lucht, R.L. Farrow, R.E. Palmer: Combust. Sci. Technol. **45**, 261 (1986)
6 G.A. Raiche, D.R. Crosley, R.A. Copeland: Am. Inst. of Phys. Proc. **191**, 758 (1989)
7 D. L'Esperance, B.A. Williams, J.W. Fleming: Combust. Flame **117**, 709 (1999)
8 K.K. Innes: J. Chem. Phys. **22**, 863 (1954)
9 J.K.G. Watson, M. Herman, J.C. Van Craen, R. Colin: J. Mol. Spectr. **95**, 101 (1982)
10 T. Suzuki, N. Hashimoto: J. Chem. Phys. **110**, 2042 (1999)
11 J.P. O'Brien, M.P. Jacobson, J.J. Sokol, S.L. Coy, R.W. Field: J. Chem. Phys. **108**, 7100 (1998)
12 M.J. Bramley, S. Carter, N.C. Handy, I.M. Mills: J. Mol. Spectr. **157**, 301 (1993)
13 T.A. Holme, R.D. Levine: J. Chem. Phys. **89**, 3379 (1988)
14 J.C. Stephenson, J.A. Blazy, D.S. King: Chem. Phys. **85**, 31 (1984)
15 R. Dopheide, W. Cronrath, H. Zacharias: Chem. Phys. Lett. **222**, 191 (1994)
16 D. Wolff, H. Zacharias: Chem. Phys. Lett. **174**, 563 (1990)
17 J.B. Jeffries, D.R. Crosley, I.J. Wysong, G.P. Smith: Proc. Combust. Inst. **23**, 1847 (1990)
18 U. Westblom, F. Fernandez-Alonso, C.R. Mahon, G.P. Smith, J.B. Jeffries, D.R. Crosley: Combust. Flame **99**, 261 (1994)